Estimation of Sphere-Size Distributions in Two-Phase Polymeric Materials from Transmission Electron Microscopy Data

W. GLEINSER, D. MAIER, M. SCHNEIDER, J. WEESE,* CHR. FRIEDRICH, and J. HONERKAMP

Freiburger Materialforschungszentrum, Stefan-Meier-Str. 31a, D-79104 Freiburg im Breisgau, Germany

SYNOPSIS

The blending of two immiscible polymer samples can lead to spherical inclusions of one component in a matrix of the other component. The mechanical solid-state properties as well as the flow behavior of the melt depend on the size of the spheres in the blend. For that reason, the sphere-size distribution is of major interest. Information about this distribution is often obtained by analyzing thin slices of the blend with transmission electron microscopy. In that way, however, the sphere-size distribution itself is not obtained. The reconstruction of the sphere-size distribution is introduced as a stereological problem, well known in fields as metallurgy, biology, geology, and medicine. It is shown that the sphere-size distribution can be reconstructed using a regularization method as implemented in the program FTIKREG. © 1994 John Wiley & Sons, Inc.

INTRODUCTION

Many polymeric materials consist of two or more immiscible polymers. In most of these materials, one component builds a matrix in which particles of the other components are embedded. In the case of two-phase materials, the particles are often approximately spheres randomly dispersed in the matrix. Two well-known examples are rubber-toughened polymers like high-impact polystyrene[1,2] and polymer blends of two immiscible thermoplastics.[3-6]

Naturally, all the particles do not have the same size and a sphere-size distribution must be used to characterize them. This distribution depends on the conditions during the preparation of the material. It influences the mechanical solid-state properties[7-10] as well as the flow behavior of the melt.[11-13] For that reason, the sphere-size distribution is of major interest and many experimental methods have been developed to characterize it.

One widespread method to obtain this morphological information is miscroscopy, especially transmission electron microscopy (TEM). To study a polymer blend with TEM, thin slices of 50–200 nm thickness have to be prepared, whereas typical particle radii range from about 50 nm up to several micrometers. Obviously, only a two-dimensional profile of the three-dimensional structure can be observed with TEM: Image-analysis of thin slices yields the radii of profiles of the particles rather than the radii of the spherical particles themselves.

Similar problems arise in metallurgy, biology, geology, and medicine. Out of the common interest in such problems, the discipline of stereology was founded in the 1960s. In general, stereology deals with mathematical problems concerning the determination of parameters characterizing a three-dimensional structure from data obtained by studying two-dimensional profiles.[14,15] The reconstruction of sphere-size distributions from so-called profile size distributions is a well-known problem in stereology and many scientists have dealt with the derivation of the relation between both distributions and with methods for reconstructing sphere-size distributions.[16-26]

In this contribution, we show that stereological results and methods can successfully be applied in polymer physics in order to determine the size dis-

Journal of Applied Polymer Science, Vol. 53, 39–50 (1994)
 CCC 0021-8995/94/010039-12

tribution of spherical inclusions in two-phase polymeric materials from TEM data. The basis of our considerations is the well-known relation between the profile-size distribution and the corresponding sphere-size distribution that is presented in the second section. Though there have been developed a large number of different methods for the numerical calculation of the sphere-size distribution,[23,25,26] we propose a new method based on Tikhonov regularization.[27] The reason for this proceeding, the advantages of this method, as well as the method itself are explained in the third section. In the fourth section, simulated data are used to show that the regularization method is an appropriate method for solving this problem. Finally, results for the sphere-size distribution of a specific polymer sample are presented in the fifth section.

RELATION BETWEEN PROFILE-SIZE AND SPHERE-SIZE DISTRIBUTIONS

In the Introduction it was noted that often thin slices of a polymer blend are studied with TEM to obtain information about the size of the spherical inclusions in the matrix. However, if a center of a sphere is outside the slice, the radius of the disc observed with TEM is smaller than the radius of the corresponding sphere. For that reason, the radii obtained with TEM provide no direct information about the sphere-size distribution: They are realizations of another distribution, the so-called profile-size distribution.

A relation between the profile-size distribution and the sphere-size distribution can be derived under the following assumptions[26]:

- The particles are distributed randomly and homogeneously.
- The particles are opaque.
- Overlapping particles can be neglected.
- Effects due to the rim of the slice can be neglected.

Denoting the profile-size distribution by $p(r)$ and the sphere-size distribution by $q(R)$ and introducing the average particle radius,

$$\bar{R} = \int_0^\infty Rq(R)\, dR \qquad (1)$$

and the thickness d of the slice, this relation can be written as

$$p(r) = \frac{d}{d + 2\bar{R}} q(r) + \frac{2r}{d + 2\bar{R}} \int_r^\infty \frac{1}{\sqrt{R^2 - r^2}} q(R)\, dR \qquad (2)$$

The first term in this equation is caused by particles with the center inside the slice. For these particles, the true particle radii are obtained. The second term is due to particles cut by the slice, but with the center outside the slice. For these particles, radii smaller than the true radii are measured.

Figure 1 shows a narrow sphere-size distribution and the corresponding profile-size distribution for varying thickness d of the slice. For $d \gg 2\bar{R}$, both distributions are nearly identical. For $d \ll 2\bar{R}$, the deviation between both distributions becomes maximal. As the average profile radius

$$\bar{r} = \int_0^\infty rp(r)\, dr \qquad (3)$$

is often used as a first approximation for the average particle radius $\bar{R}$, it is also interesting to compare both quantities (Table I). For $d \gg 2\bar{R}$, the values for both quantities are nearly the same. For $d \ll 2\bar{R}$, the average profile radius $\bar{r}$ is about 20% smaller than the average particle radius $\bar{R}$.

RECONSTRUCTION OF SPHERE-SIZE DISTRIBUTIONS

Until now, a large number of methods for reconstructing sphere-size distributions have been developed.[23,25,26] The starting point of a variety of these methods is a histogram for the profile-size distribution. Then, eq. (2) is replaced by a discrete approximation and, finally, the resulting linear equations are solved. Alternatively, eq. (2) is solved analytically and the discrete approximation is introduced after analytical inversion.

There is, however, a serious drawback inherent in these methods: Especially in the case of infinitely thin slices ($d = 0$), the condition number of the resulting linear equations increases with increasing number of points where the sphere-size distribution is calculated; these methods are extremely sensitive to statistical errors in the histogram.[23]

The bad behavior of the condition number is a typical property of linear equations derived by discretization of an integral equation of the first kind. As these equations have several bad properties, the

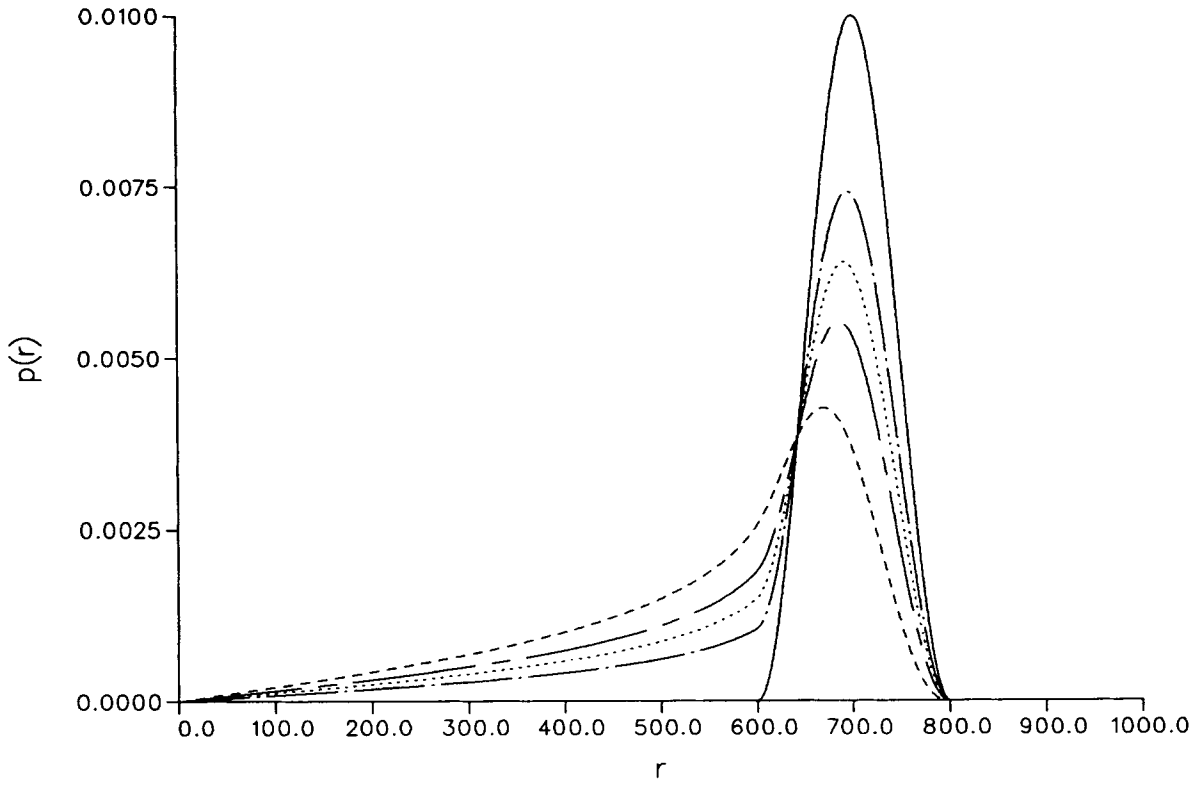

Figure 1 Narrow sphere-size distribution (solid line) and the corresponding profile-size distributions for varying thickness d of the slice: (dashed) $d = 0$; (chain dashed) $d = 500$; (dotted) $d = 1000$; (chain dotted) $d = 2000$. For $d = \infty$, the sphere-size distribution and the corresponding profile-size distribution are identical.

inversion of such an equation is called an ill-posed problem. Specific methods, the so-called regularization methods, have been developed by mathematicians for the calculation of stable solutions of such problems.[27-30] For that reason, we propose to use a regularization method for reconstructing sphere-size distributions.

Table I Average Profile Radii $\bar{r}$ of the Distributions of Figure 1

d	$\bar{r}$	$\bar{R}$
0	551	700
500	590	700
1000	613	700
2000	638	700
∞	700	700

These distributions characterize the profile-size distributions corresponding to a narrow sphere-size distribution with average particle radius $\bar{R}$ for varying thickness d of the slice.

The starting point for the regularization method is a histogram for the profile-size distribution $p(r)$ with n bins:

$$p_h(r) = p_i^\sigma;\ r \in]r_i - h, r_i + h];\quad i = 1, \ldots, n \tag{4}$$

with

$$h = \frac{r_{max} - r_{min}}{2n} \tag{5a}$$

$$r_i = r_{min} + (2i - 1)h \tag{5b}$$

$$p_i^\sigma = \frac{1}{2hm}\,\#\{r_1^\sigma, \ldots, r_m^\sigma \,|\, r_i - h < r_j^\sigma \leq r_i + h\} \tag{5c}$$

In this equation, $r_1^\sigma, \ldots, r_m^\sigma$ denote the measured profile radii. For r_{max}, a value slightly larger than $\max\{r_1^\sigma, \ldots, r_m^\sigma\}$ must be chosen. r_{min} should be

slightly larger than the radius of the smallest disc reliably resolved by TEM. $\#\mathcal{A}$ denotes the number of elements in the set $\mathcal{A}$. If h is not too large, the values p_i^q can be considered as estimates for the profile size distribution $p(r)$ at $r = r_i$. In general, the values p_i^q are estimates of the quantities

$$\bar{p}(r_i) = \frac{1}{2h}\int_{r_i-h}^{r_i+h} p(r)\,dr = \frac{1}{2h}\left[\frac{d}{d+2\bar{R}}\int_{r_i-h}^{r_i+h} q(R)\,dR + \frac{2}{d+2\bar{R}}\int_{r_i-h}^{\infty} K_h(r_i, R)q(R)\,dR\right] \quad (6a)$$

with $K_h(r, R)$ given by

$$K_h(r,R) = \begin{cases} \sqrt{R^2-(r-h)^2}; & R-h < r \le R+h \\ \sqrt{R^2-(r-h)^2} & \\ -\sqrt{R^2-(r+h)^2}; & r \le R-h \end{cases} \quad (6b)$$

To apply a regularization method in addition to the estimates p_i^q, quantities σ_i^2 characterizing the variances of the estimates are needed. Assuming Poisson statistics, the variances can be calculated according to

$$\sigma_i^2 = \frac{1}{2hm}p_i^q \quad (7)$$

For $2hmp_i^q < 3$, the variance σ_i^2 of eq. (7) can be misleading and the corresponding estimate p_i^q would have a too large influence on the result calculated by regularization. For that reason, expression (7) is replaced by

$$\sigma_i^2 = \frac{3}{(2hm)^2} \quad (8)$$

in this case.

With Tikhonov regularization, an estimate $\tilde{q}_\lambda^q(R)$ for the scaled sphere-size distribution

$$\tilde{q}(R) = q(R)/(d+2\bar{R}) \quad (9)$$

can be obtained for $r_{\min} \le R \le r_{\max}$. Introducing the so-called regularization parameter λ and denoting the second derivative of $\tilde{q}(R)$ by $\tilde{q}''(R)$, this estimate can be determined by minimizing

$$V(\lambda) = \sum_{i=1}^{n}\frac{1}{\sigma_i^2}\left[p_i^q - \frac{1}{2h}\left(d\int_{r_i-h}^{r_i+h}\tilde{q}(R)\,dR + 2\int_{r_i-h}^{r_{\max}} K_h(r_i, R)\tilde{q}(R)\,dR\right)\right]^2 + \lambda\int_{r_{\min}}^{r_{\max}}[\tilde{q}''(R)]^2\,dR \quad (10)$$

with respect to $\tilde{q}(R)$. Additionally, the constraints

$$\tilde{q}(R) \ge 0 \quad (11)$$

must be taken into account, because the sphere-size distribution is positive. With an appropriate value for the regularization parameter λ, the first term on the right-hand side of eq. (10) forces the result to be compatible with the data. The second term leads to a smooth estimate $\tilde{q}_\lambda^q(R)$. The desired estimate $q_\lambda^q(R)$ for the sphere-size distribution $q(R)$ itself is obtained by normalization of the estimate $\tilde{q}_\lambda^q(R)$:

$$q_\lambda^q(R) = \frac{\tilde{q}_\lambda^q(R)}{\int_0^\infty \tilde{q}_\lambda^q(R)\,dR} \quad (12)$$

The calculations in connection with Tikhonov regularization have been performed with the program FTIKREG,[31] which has been developed by one of the authors. Given noisy experimental data and the corresponding data errors, the program FTIKREG computes the approximate solution of equations analogous to eq. (2) defined by Tikhonov regularization. In addition, FTIKREG offers several features, such as the ability to estimate the optimal value of the regularization parameter λ with the SC method.[32] This feature is very important, because it depends mainly on this parameter, whether the result obtained by a regularization method is good or not.

TESTING THE METHOD WITH SIMULATED DATA

As a first example, the sphere-size distribution of Figure 2(b) (full line) was considered. For this distribution, 1000 profiles with a distribution given by eq. (2) ($d = 500$) were generated. To simulate the finite resolution of TEM, all profiles with $r_i^q < 200$ were discarded. The histogram obtained from the remaining profiles with $r_{\min} = 200$, $r_{\max} = 800$ and $n = 20$ is shown in Figure 2(a). Given the histogram, the sphere-size distribution was calculated with FTIKREG as described in the preceding section.

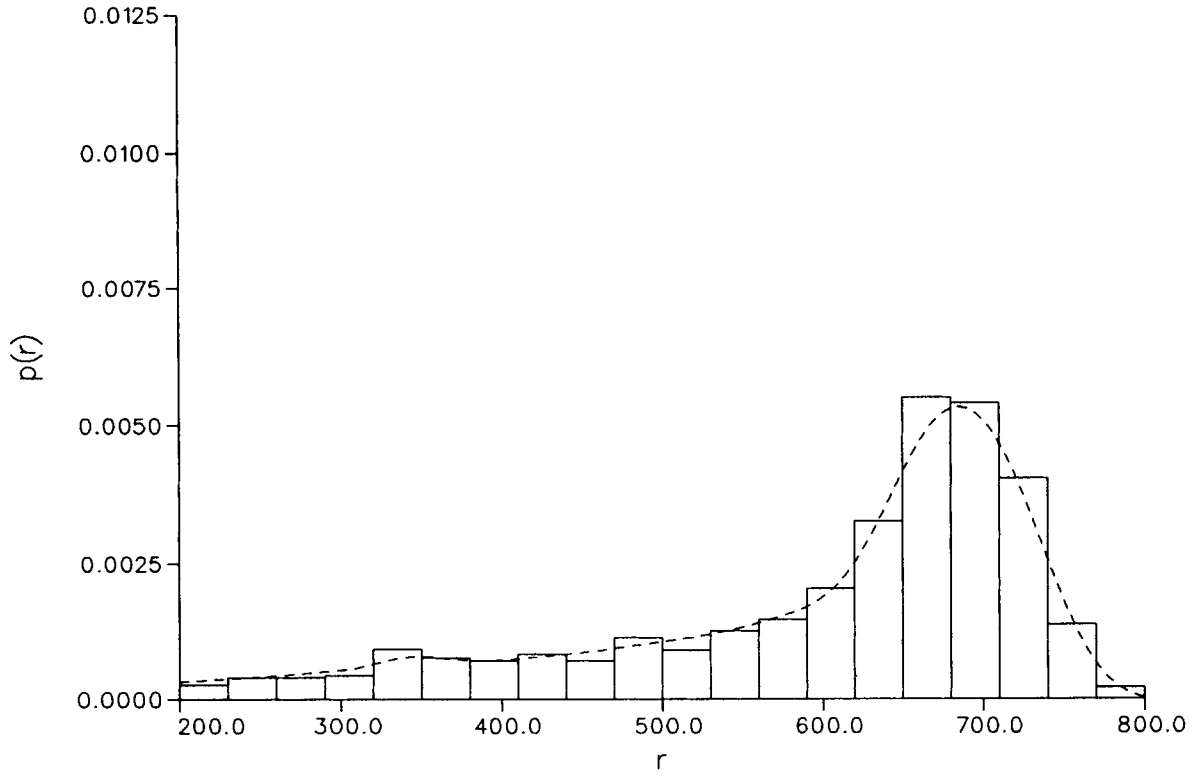

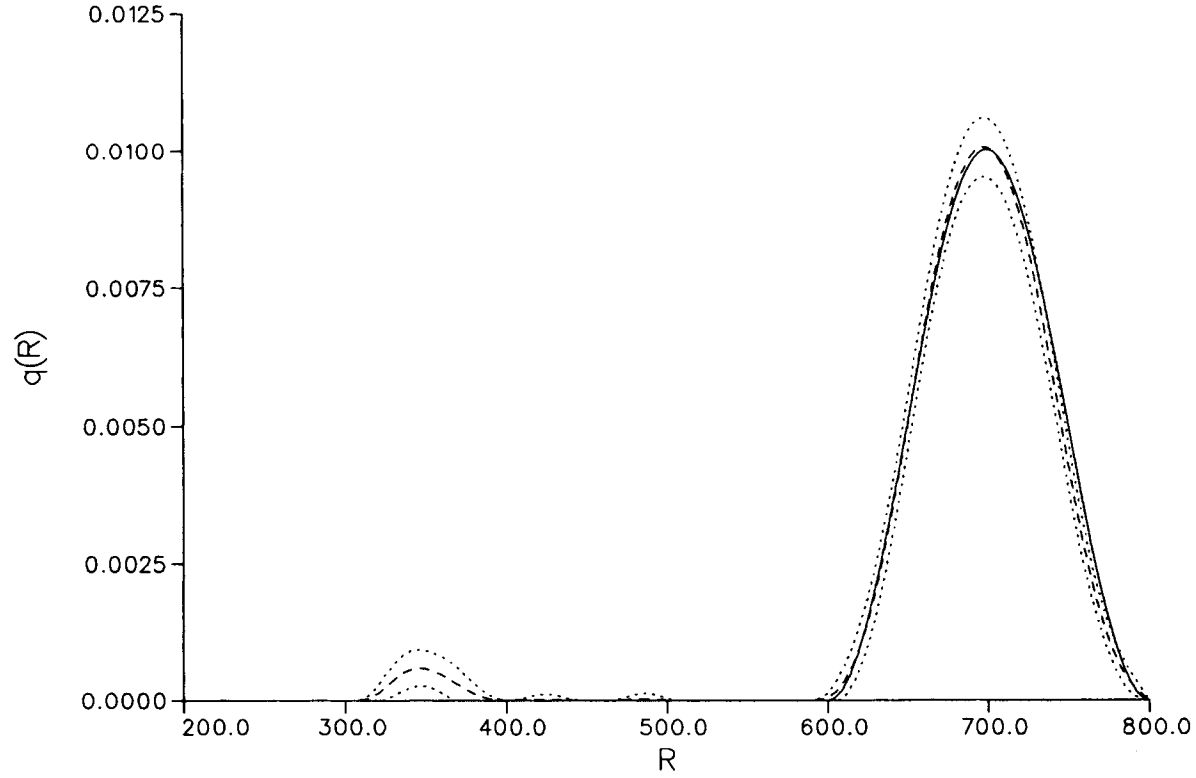

Figure 2 (a) Histogram calculated with $r_{min} = 200$, $r_{max} = 800$, and $n = 20$ from the 1000 profiles of example 1. The dashed line marks the values for the profile-size distribution recalculated from the sphere-size distribution obtained by regularization. (b) Sphere-size distribution obtained by regularization (dashed line). The dotted line characterizes the statistical error of the reconstructed distribution. The solid line marks the original sphere-size distribution.

Figure 2(b) shows that the result is in excellent agreement with the original distribution: The large peak at $R = 700$ is reconstructed very well. For smaller values of R, the result indicates another contribution. The dotted curves characterizing the influence of the data errors on the result indicate, however, that this contribution is statistically insignificant. The values calculated for the average particle radius (Table II) are also in good agreement with the true value for this quantity.

Of course, the question arises whether the reconstructed sphere-size distribution depends strongly on the number n of the histogram's bins. To answer this question, the calculations have been repeated with $n = 10$, 20, 50, and 100. The results presented in Figure 3 illustrate that for a reasonable choice of the number of bins the reconstructed sphere-size distribution is nearly independent of this quantity. The values for the average particle radius also do not show a strong dependence on this quantity.

Good results were also obtained when reconstructing a sphere-size distribution with two well-separated peaks. It is more difficult to reconstruct a distribution with two peaks that are near to each other. To illustrate this, 1000 profiles for the sphere-size distribution of Figure 4(b) (full line) were generated ($d = 200$). Again, the finite resolution of TEM was simulated by discarding profiles with $r_i^v < 200$. The histogram calculated from the remaining profiles with $r_{min} = 200$, $r_{max} = 900$, and $n = 20$ is shown in Figure 4(a). In this example, the result calculated with regularization is not as good as in the first example: Though the original sphere-size distribution is bimodal, the reconstructed sphere-size distribution shows only one broad peak [Fig. 4(b)]. Nearly identical results are obtained when

Table II Average Particle Radii $\bar{R}$ of the Sphere-size Distributions of Figure 3

n	$\bar{R}$
10	687.96
20	688.79
50	689.00
100	685.19
Exact	700.00

These distributions have been reconstructed from histograms with n bins.

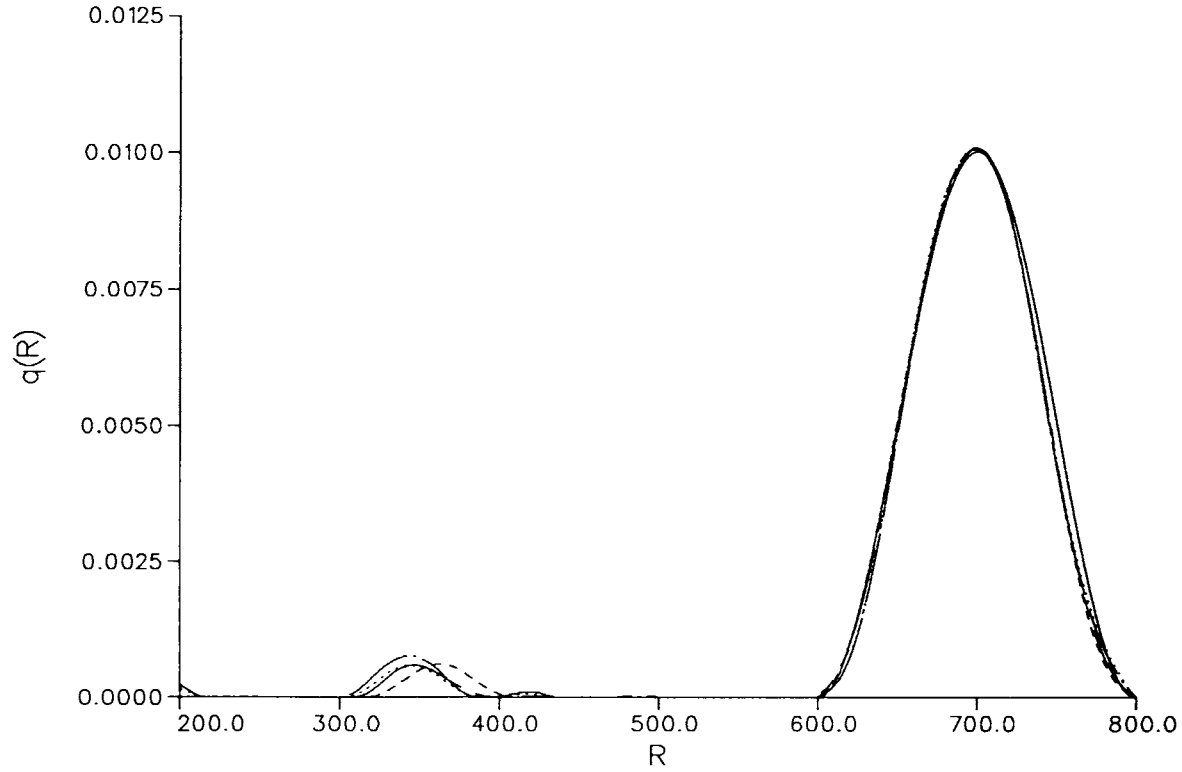

Figure 3 Sphere-size distribution reconstructed from histograms with (dashed) $n = 10$, (chain dashed) $n = 20$, (dotted) $n = 50$, and (chain dotted) $n = 100$ bins. The solid line marks the original sphere-size distribution.

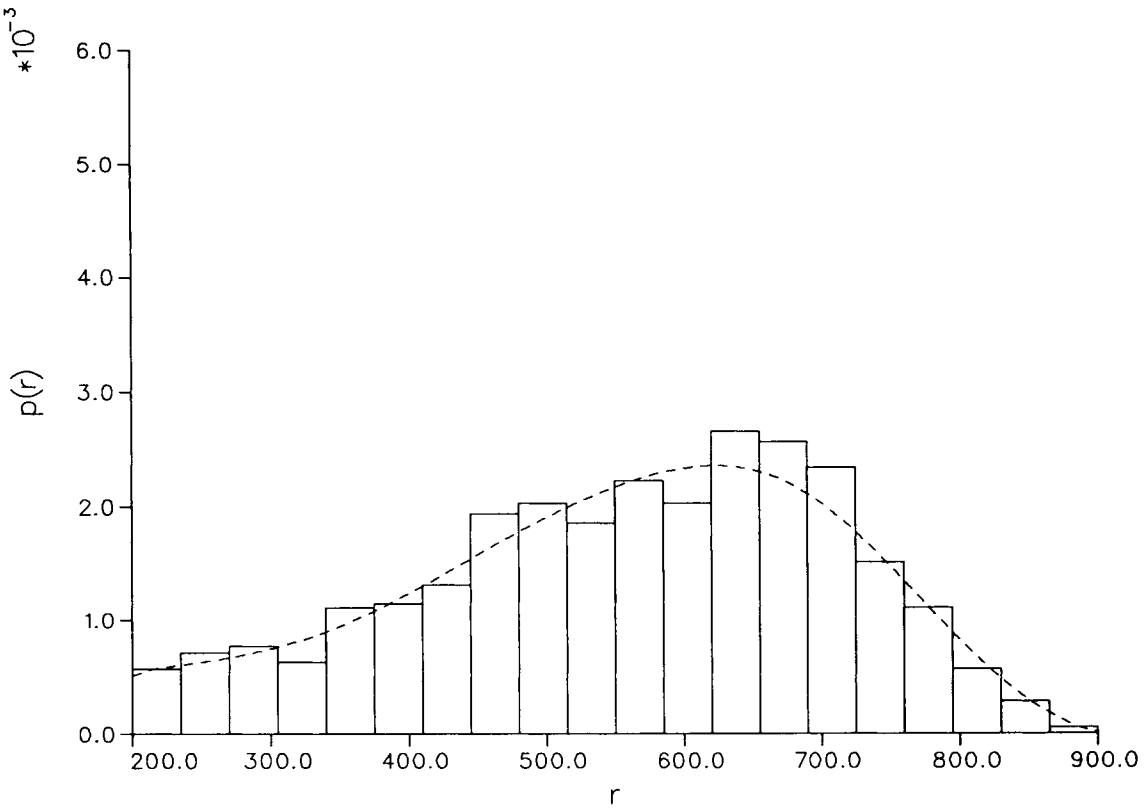

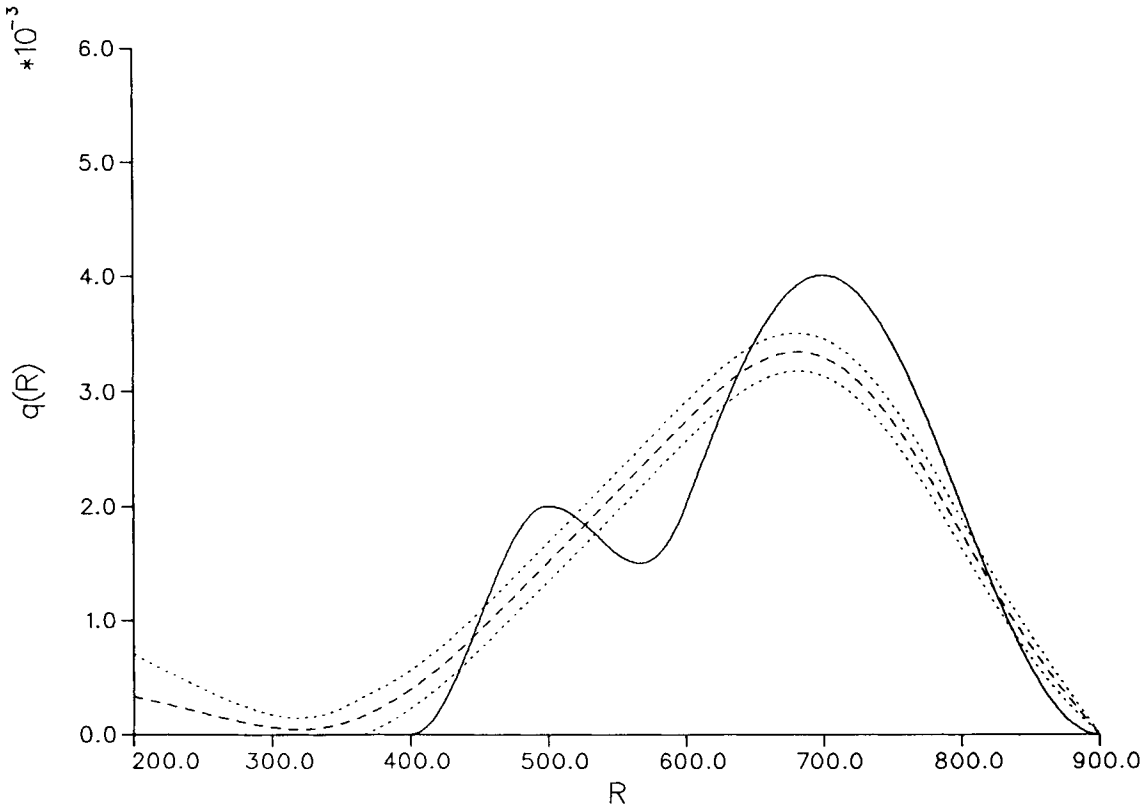

Figure 4 (a) Histogram calculated with $r_{min} = 200$, $r_{max} = 900$, and $n = 20$ from the 1000 profiles of example 2. The dashed line marks the values for the profile-size distribution recalculated from the sphere-size distribution obtained by regularization. (b) Sphere-size distribution obtained by regularization (dashed line). The dotted line characterizes the statistical error of the reconstructed distribution. The solid line marks the original sphere-size distribution.

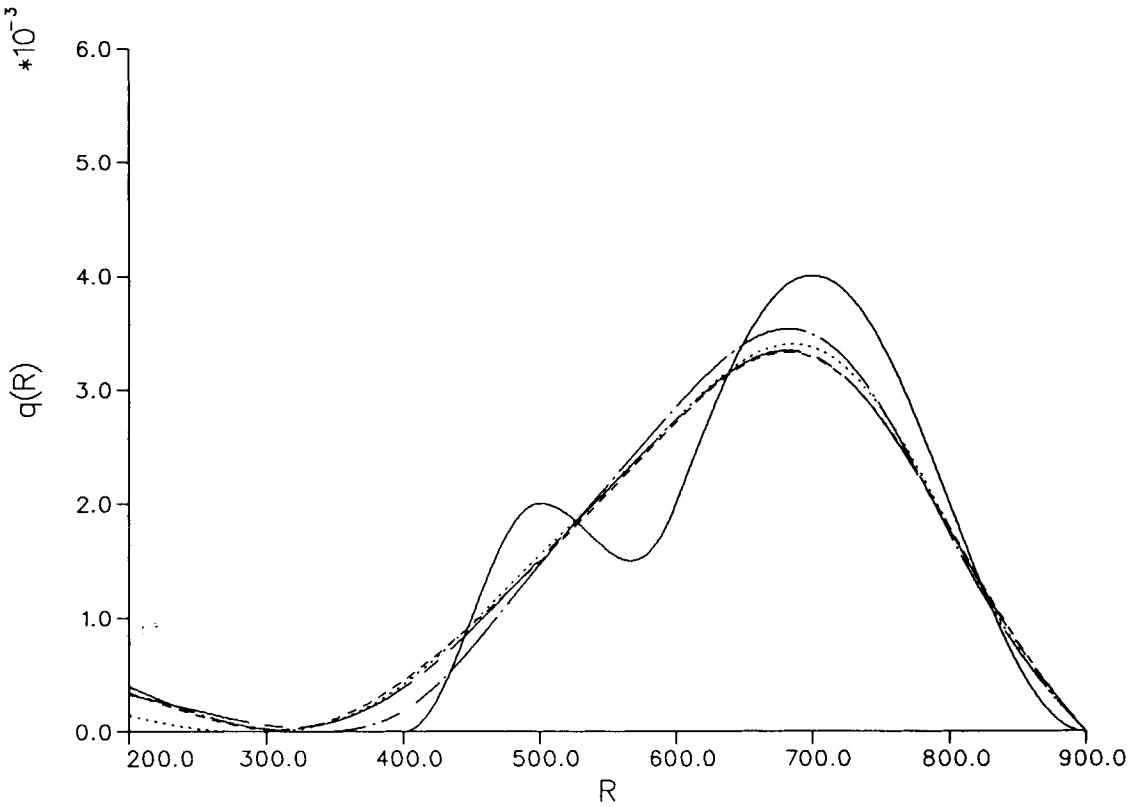

Figure 5 Sphere-size distribution reconstructed from histograms with (dashed) $n = 10$, (chain dashed) $n = 20$, (dotted) $n = 50$, and (chain dotted) $n = 100$ bins. The solid line marks the original sphere-size distribution.

varying the number n of the histogram's bins (Fig. 5).

The reconstructed sphere-size distribution becomes more accurate with an increasing number of the available profiles. This is illustrated in the last example where the sphere-size distribution of the preceding example is reconstructed from 5000 profiles. The histogram calculated with $r_{min} = 200$, $r_{max} = 900$, and $n = 100$ and the results obtained by regularization are shown in Figure 6: Though the result for the small peak is not very good, the regularization method leads to a bimodal distribution. For this example, the calculations have also been repeated with different values of the number n of the histogram's bins. As before, there is a large range where the results (Fig. 7) are nearly independent of this quantity.

The examples above lead to the following conclusions concerning the properties of the proposed regularization method:

- Given m profiles, the number n of the histogram's bins should be chosen according to

$$m/50 \leq n \leq m/20 \qquad (13)$$

For this choice, the reconstructed sphere-size distribution is nearly independent of this quantity.

- The reconstructed sphere-size distribution becomes more accurate with an increasing number of the available profiles.
- The quality of the result depends on the width of the peaks and the distance between the peaks. To reconstruct a distribution with two well-separated peaks, fewer profiles are needed than for the reconstruction of a distribution with two peaks that are near to each other.

APPLICATION TO EXPERIMENTAL DATA

Experimental data have been obtained from a material consisting of cross-linked polystyrene microparticles with a grafted poly(2-vinylpyridine) shell embedded in an epoxy resin matrix.[33]

The microparticles were prepared by sequential anionic dispersion polymerization of styrene/divinylbenzene and 2-vinylpyridine in n-heptane with

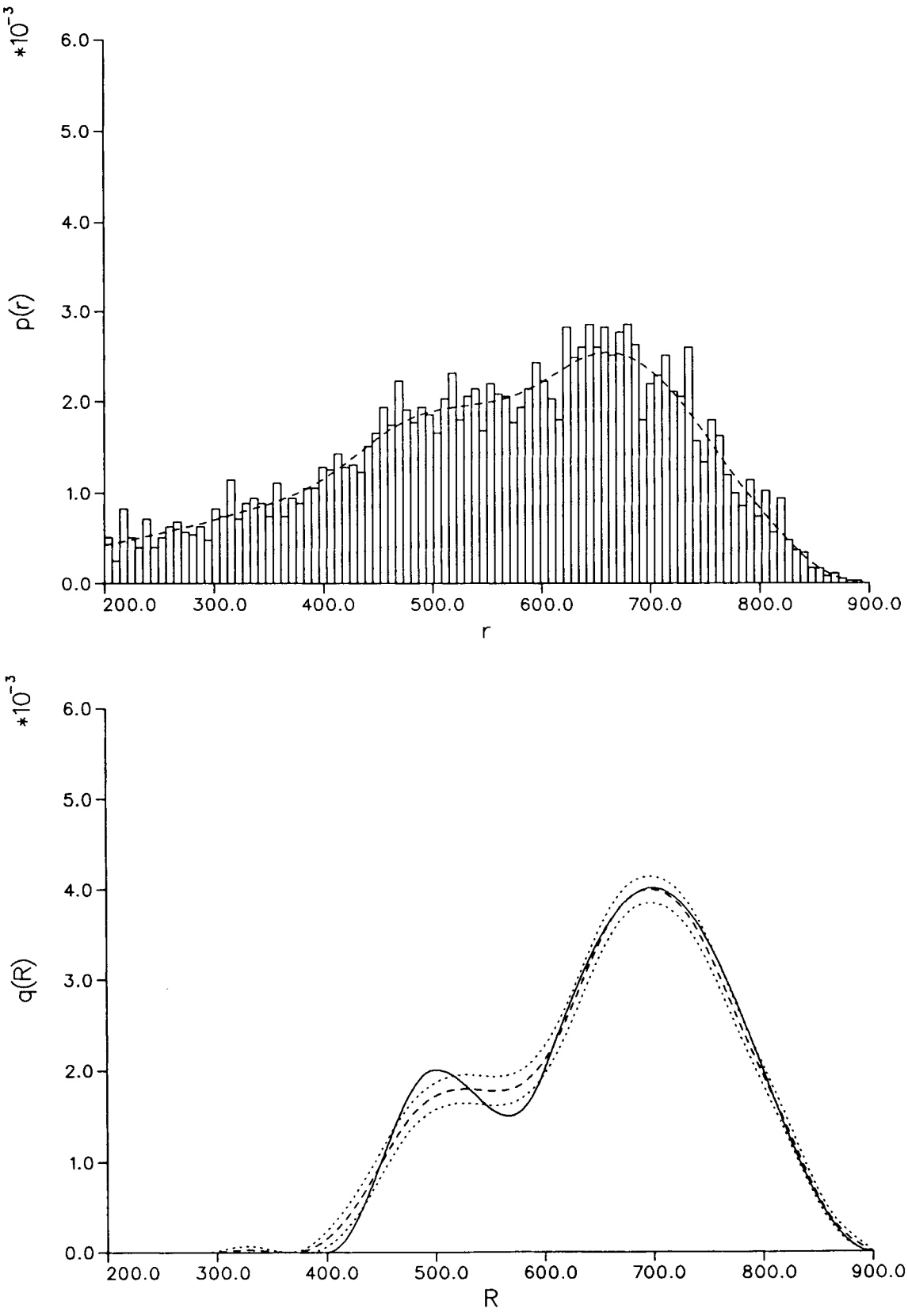

Figure 6 (a) Histogram calculated with r_{min} = 200, r_{max} = 900, and n = 100 from the 5000 profiles of example 3. The dashed line marks the values for the profile-size distribution recalculated from the sphere-size distribution obtained by regularization. (b) Sphere-size distribution obtained by regularization (dashed line). The dotted line characterizes the statistical error of the reconstructed distribution. The solid line marks the original sphere-size distribution.

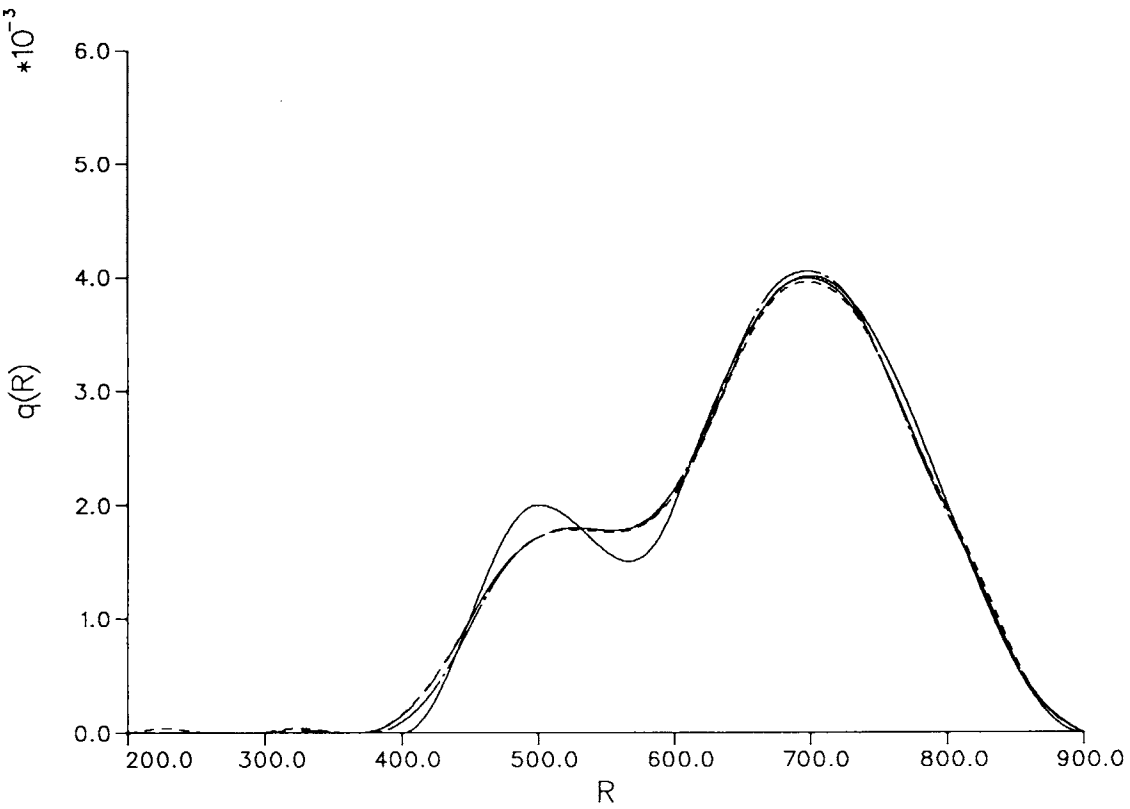

Figure 7 Sphere-size distribution reconstructed from histograms with (dashed) $n = 50$, (chain dashed) $n = 100$, (dotted) $n = 250$, and (chain dotted) $n = 500$ bins. The solid line marks the original sphere-size distribution.

sec-butyllithium as the initiator. In the first step, Kraton G 1650 (Shell), a triblock copolymer with two polystyrene endblocks and a hydrogenated polybutadiene block, was used as the polymeric stabilizer. In the second step, the 2-vinylpyridine was added to the "living" polystyrene particles after modification of the carbanions with 1,1-diphenylethylene. After termination with methanol, the particles were precipitated in petrolether, and extracted with methanol. The freeze-dried particles were redispersible in tetrahydrofurane. A 0.50/0.50 weight ratio of styrene and 2-vinylpyridine was determined independently by nitrogen elemental analysis and gravimetric yield calculations.

After embedding the particles in an epoxy resin matrix, ultrathin specimens were obtained by a Reichert-Jung Ultracut-E microtome with a diamond knife at room temperature. The thickness of the specimen was about 60 nm, indicated by their colorless-to-silvery interference. No particles were removed from the matrix during the cutting process, due to the possible reaction of the pyridine groups of the poly(2-vinylpyridine) blocks with the epoxy groups, resulting in a better phase adhesion.

The images were obtained by a Zeiss CEM 902 electron microscope, using an acceleration voltage of 80 kV and a hairpin tungsten filament as the electron source. The radii of the profiles in the ultrathin specimen were determined with an IBAS 2000 image processing system.

Altogether, 1381 profiles with radii between 75 and 1100 nm were measured. Given the profiles, a histogram was calculated using the parameters r_{min} = 80 nm, r_{max} = 1100 nm, and $n = 50$ [Fig. 8(a)]. The sphere-size distribution obtained by regularization [Fig. 8(b)] is unimodal, as was expected from the preparation of the microparticles. Most of the particles have radii between 300 and 1100 nm. The average particle radius is given by 692 nm and the most frequent particle radius is about 770 nm.

CONCLUSIONS

The determination of sphere-size distributions from profiles observed with TEM in a thin slice has been introduced as a stereological problem. For solving this problem, a two-step method has been proposed.

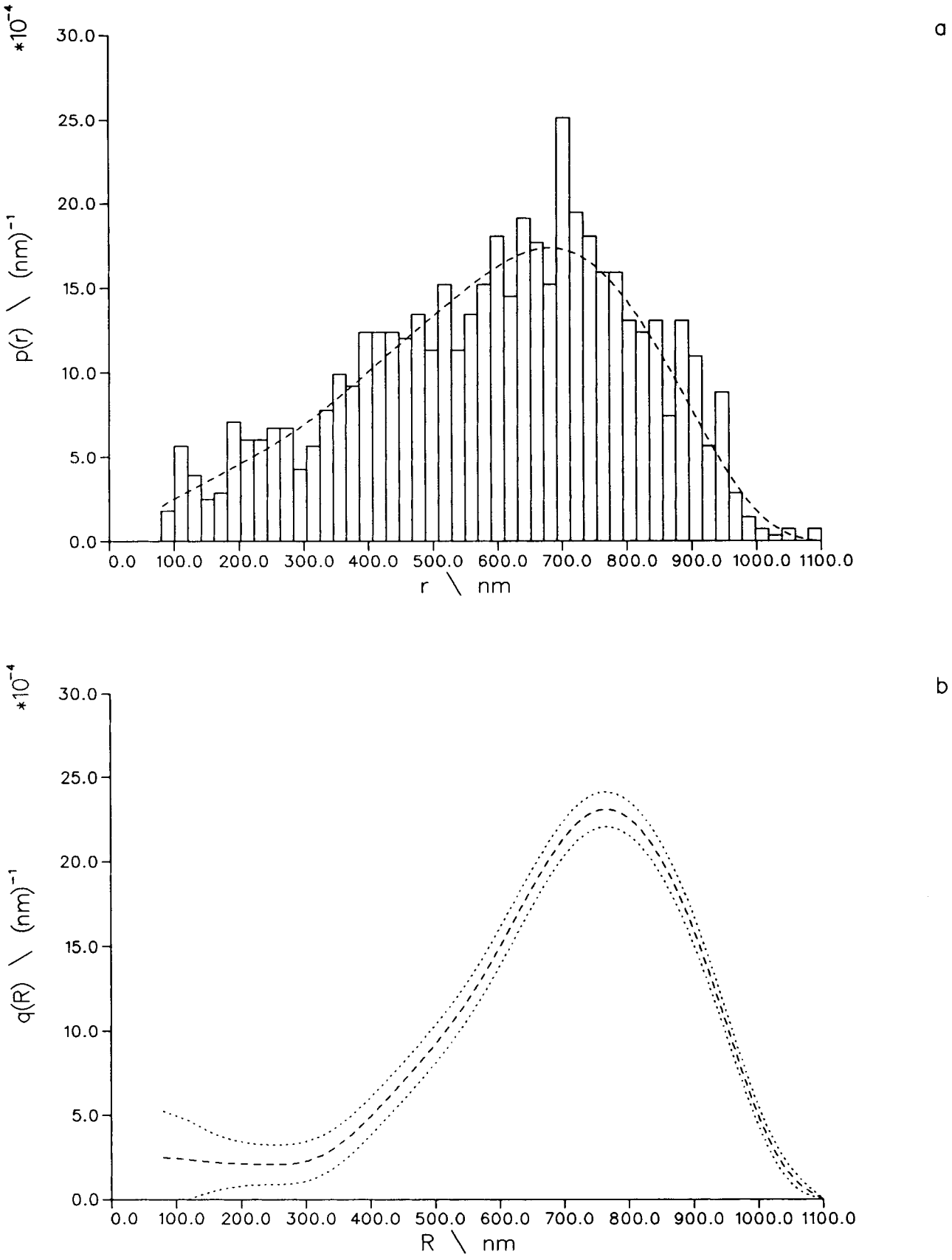

Figure 8 (a) Histogram calculated with $r_{min} = 80$, $r_{max} = 1100$, and $n = 50$ from the 1381 profiles of the cross-linked polystyrene microparticles. The dashed line marks the values for the profile-size distribution recalculated from the sphere-size distribution obtained by regularization. (b) Sphere-size distribution obtained by regularization (dashed line). The dotted line characterizes the statistical error of the reconstructed distribution.

In the first step, a histogram for the profile-size distribution is calculated. In the second step, a regularization method is used to reconstruct the sphere-size distribution from the histogram.

Using simulated data, it has been illustrated that this method is appropriate for reconstructing sphere-size distributions. In addition, the simulations have shown that the number of the histogram's bins has no crucial influence on the result and that the result becomes more accurate with an increasing number of measured profile radii. To demonstrate the practical applicability, the regularization method has been used to estimate the sphere-size distribution of cross-linked polystyrene microparticles with a grafted poly(2-vinylpyridine) shell embedded in an epoxy resin matrix.

D. M. would like to acknowledge the financial support by Rheometrics Inc., Piscataway, New Jersey.

REFERENCES

1. C. B. Bucknall, *Toughened Plastics,* Applied Science, London, 1977.
2. A. Echte, in *Rubber Toughened Plastics,* C. K. Riew, Ed., American Chemical Society, Washington, DC, 1989.
3. C. H. Burns and W. N. Kim, *Polym. Eng. Sci.,* **28,** 1362 (1988).
4. D. Graebling and R. Muller, *J. Rheol.,* **34,** 193 (1990).
5. Y. Tokeda and D. R. Paul, *J. Polym. Sci. Part B Polym. Phys.,* **30,** 1273 (1992).
6. W. Gleinser, H. Braun, Chr. Friedrich, and H.-J. Cantow, *Polymer,* **35,** 128 (1994).
7. A. M. Donald and E. J. Kramer, *J. Appl. Polym. Sci.,* **27,** 3729 (1982).
8. S. Y. Hobbs, *Polym. Eng. Sci.,* **26,** 74 (1986).
9. G. Cigna, P. Lomellini, and M. Merlotti, *J. Appl. Polym. Sci.,* **37,** 1527 (1989).
10. R. A. Hall, *J. Mater. Sci.,* **27,** 6029 (1992).
11. S. J. Choi and W. R. Schowalter, *Phys. Fluids,* **18,** 420 (1975).
12. J.-F. Palierne, *Rheol. Acta,* **29,** 204 (1990).
13. D. Graebling, R. Muller, and J.-F. Palierne, *Macromolecules,* **26,** 320 (1990).
14. E. E. Underwood, *Quantitative Stereology,* Addison-Wesley, Reading, MA, 1970.
15. E. R. Weibel, *Stereological Methods,* Academic Press, New York, 1979.
16. S. D. Wicksell, *Biometrika,* **17,** 84 (1925).
17. S. D. Wicksell, *Biometrika,* **18,** 151 (1926).
18. H. Elias, *Z. Wiss. Mikrosk.,* **62,** 32 (1954).
19. F. Lenz, *Z. Wiss. Mikrosk.,* **63,** 50 (1956).
20. G. Bach, *Z. Wiss. Mikrosk.,* **64,** 265 (1959).
21. G. Bach, *Z. Wiss. Mikrosk.,* **65,** 285 (1963).
22. P. L. Goldsmith, *Br. J. Appl. Phys.,* **18,** 813 (1967).
23. R. S. Anderssen and A. J. Jakeman, *J. Microsc.,* **105,** 135 (1975).
24. R. Coleman, *Biomet. J.,* **24,** 273 (1982).
25. L. M. Cruz-Orive, *J. Microsc.,* **131,** 265 (1983).
26. K. Kanatani and O. Ishikawa, *J. Comput. Phys.,* **57,** 229 (1985).
27. C. W. Groetsch, *The Theory of Tikhonov Regularization for Fredholm Equations of the First Kind,* Pitman, London, 1984.
28. M. Bertero, in *Inverse Problems,* G. Talenti, Ed., Springer-Verlag, Berlin, 1986.
29. A. K. Louis, *Inverse und schlecht gestellte Probleme,* Teubner Studienbücher, Stuttgart, 1989.
30. H. W. Engl, *Surv. Math. Ind.,* **3,** 71 (1993).
31. J. Weese, *Comput. Phys. Commun.,* **69,** 99 (1992).
32. J. Honerkamp and J. Weese, *Cont. Mech. Therm.,* **2,** 17 (1990).
33. M. Schneider, PhD Thesis, Universität Freiburg, to appear.

Received August 26, 1993
Accepted December 23, 1993